Slc25a13-Knockout Mice Harbor Metabolic Deficits but Fail To Display Hallmarks of Adult-Onset Type II Citrullinemia

David S. Sinasac,[1,2] Mitsuaki Moriyama,[3] M. Abdul Jalil,[4,5] Laila Begum,[4] Meng Xian Li,[4]
Mikio Iijima,[4] Masahisa Horiuchi,[4] Brian H. Robinson,[6] Keiko Kobayashi,[4]
Takeyori Saheki,[4] and Lap-Chee Tsui[1,2,7]*

*Genetics & Genomic Biology[1] and Metabolism Research Programs,[6] The Hospital for Sick Children, Toronto, Ontario,
Canada M5G 1X8; Department of Molecular & Medical Genetics, University of Toronto, Toronto, Ontario, Canada
M5S 1A8[2]; Laboratory of Integrative Physiology in Veterinary Sciences, Osaka Prefecture University, Sakai, Osaka
599-8531[3] and Department of Molecular Metabolism & Biochemical Genetics[4] and Laboratory for
Neuroanatomy,[5] Kagoshima University Graduate School of Medical & Dental Sciences, Kagoshima
890-8520, Japan; and The University of Hong Kong, Hong Kong Special Administrative Region,
People's Republic of China[7]*

Adult-onset type II citrullinemia (CTLN2) is an autosomal recessive disease caused by mutations in *SLC25A13*, the gene encoding the mitochondrial aspartate/glutamate carrier citrin. The absence of citrin leads to a liver-specific, quantitative decrease of argininosuccinate synthetase (ASS), causing hyperammonemia and citrullinemia. To investigate the physiological role of citrin and the development of CTLN2, an *Slc25a13*-knockout (also known as *Ctrn*-deficient) mouse model was created. The resulting *Ctrn*$^{-/-}$ mice were devoid of *Slc25a13* mRNA and citrin protein. Liver mitochondrial assays revealed markedly decreased activities in aspartate transport and the malate-aspartate shuttle. Liver perfusion also demonstrated deficits in ureogenesis from ammonia, gluconeogenesis from lactate, and an increase in the lactate-to-pyruvate ratio within hepatocytes. Surprisingly, *Ctrn*$^{-/-}$ mice up to 1 year of age failed to show CTLN2-like symptoms due to normal hepatic ASS activity. Serological measures of glucose, amino acid, and ammonia metabolism also showed no significant alterations. Nitrogen-loading treatments produced only minor changes in the hepatic ammonia and amino acid levels. These results suggest that citrin deficiency alone may not be sufficient to produce a CTLN2-like phenotype in mice. These observations are compatible, however, with the variable age of onset, incomplete penetrance, and strong ethnic bias seen in CTLN2 where additional environmental and/or genetic triggers are now suspected.

Citrullinemia is caused by a deficiency of the urea cycle enzyme argininosuccinate synthetase (ASS; EC 6.3.4.5), which catalyzes the ligation reaction of citrulline (Cit) and aspartate (Asp) to form argininosuccinate. The loss of ASS activity results in an accumulation of plasma Cit and ammonia in patients. Early- and late-onset forms of citrullinemia have been described clinically (24, 39). With the discovery of the gene responsible for the late-onset form (19), citrullinemia can be clearly divided into two forms: classical citrullinemia (CTLN1) (Online Mendelian Inheritance in Man [OMIM] no. 215700), caused by mutations in the ASS gene (8, 15), and adult-onset type II citrullinemia (CTLN2) (OMIM no. 603471). CTLN2 is caused by a deficiency of citrin that is encoded by the SLC25A13 gene on chromosome 7q21.3 (19, 45). The loss of citrin function leads to a liver-specific, quantitative ASS deficiency in CTLN2 patients (39–41) in which the residual amount of enzyme that is present displays normal kinetic properties (17). In addition, the expression level of *ASS* mRNA in CTLN2 patients appears to be normal (17, 18). The causal link between the absence of citrin and the hepatic loss of ASS in CTLN2 patients remains to be clarified.

The liver-specific ASS deficiency in CTLN2 patients leads to a lesser increase in plasma Cit levels than that in CTLN1 patients, proportionally elevated levels of plasma arginine (Arg), and an increase in urine argininosuccinate (36–38). Furthermore, CTLN2 patients exhibit an increase in their plasma threonine-to-serine (Thr/Ser) ratio (13, 37) as well as elevated levels of pancreatic secretory trypsin inhibitor (PSTI) in serum, the latter resulting from its up-regulated transcriptional expression in the liver (13, 16). The most characteristic feature of CTLN2 is the late onset of serious and recurring symptoms of hyperammonemia and neuropsychiatric symptoms, often leading to rapid death (14, 34, 35). Although the prognosis of CTLN2 is poor, liver transplantation is a remarkably effective therapy (11). Lastly, CTLN2 shows a strong ethnic bias, as it has been reported almost exclusively in the Japanese population, with several clinical reports implicating exposures to medication, infection, and/or stress as triggers for the onset of the disease in some CTLN2 patients (14).

Following the identification of *SLC25A13* mutations in CTLN2 patients (19), molecular diagnosis of infants has revealed that *SLC25A13* mutations also cause an idiopathic hepatitis with transient citrullinemia in neonates (3, 29, 31, 34, 47–49, 52). This newly identified disease has been dubbed neonatal intrahepatic cholestasis caused by citrin deficiency (NICCD) (OMIM no. 605814) (31, 52). Typically, NICCD is not as severe as CTLN2, with patients recovering apparently

healthy states by 1 year of age simply with regulated feeding programs. To date, 10 separate *SLC25A13* mutations have been reported in NICCD and CTLN2 patients (3, 19, 52, 53). Examination of liver biopsy specimens from patients with the most common mutations, by use of an anti-citrin antibody, has failed to detect cross-reactive material, suggesting that they represent null alleles (53). The screening of 1,372 control samples for nine separate mutations in *SLC25A13* has identified a heterozygous-gene carrier frequency of 1 in 70 in the Japanese population (34). This frequency predicts an estimated homozygous-gene carrier frequency of 1 in 20,000, which is 5 times higher than the incidence of CTLN2 calculated from consanguinity (1 in 100,000) (18) and more than 10 times higher than the reported observed frequency of CTLN2 in Japan (1 in 230,000) (27). The explanation for this discrepancy remains to be discovered.

Citrin and its isoform aralar (encoded by the paralogous gene *SLC25A12*) both represent mitochondrial Asp/glutamate (Glu) carrier (AGC) proteins (32) that share strong amino acid conservation (19). As a result, both proteins have similar characteristics of binding calcium and localizing to the inner mitochondrial membrane (6, 7, 10, 14, 32). Their tissue expression patterns, however, are quite distinct. In both humans and mice, citrin is expressed predominantly in the liver, kidney, and heart, whereas the expression of aralar is highest in skeletal muscle, brain, and heart (2, 6, 10, 19). This difference in tissue expression patterns is important for citrin deficiency (encompassing both NICCD and CTLN2), a liver-specific disorder, as the two isoforms presumably represent functionally equivalent proteins. Therefore, with citrin representing the major AGC in the liver, the various symptoms of citrin deficiency may be understood as resulting from a defect in the export of mitochondrial Asp, with the loss of hepatic ASS contributing to the symptoms of CTLN2 (34).

Citrin and aralar, functioning as AGCs, are implicated in metabolic compartmentation in the context of playing significant roles in (i) the transfer of reducing equivalents into mitochondria for the generation of ATP by oxidative phosphorylation via the malate (Mal)-Asp NADH shuttle (4), (ii) exporting Asp as a substrate for phosphoenolpyruvate formation and the creation of glucose from 3-carbon precursors such as lactate and gluconeogenic amino acids (20), (iii) preferentially providing intramitochondrial Asp for the formation of argininosuccinate during the urea cycle (25), and (iv) establishing an equilibrium that maintains a difference between the cytosolic and mitochondrial NADH/NAD redox states (51). Furthermore, these processes vary in their importance in different tissues, ranging from an also ubiquitous need for the importation of NADH generated during glycolysis and the maintenance of cellular redox equilibrium in most tissues, to the processes of gluconeogensis and ureogenesis, which occur primarily and solely within the liver, respectively. Although one would expect all of these processes to be affected by the loss of citrin, a number of important questions regarding citrin deficiency remain to be resolved; these include the extent to which the AGC-dependent pathways are perturbed by citrin's absence, the nature of citrin's maintenance of hepatic ASS protein levels, and the enhanced expression of hepatic PSTI seen in CTLN2 patients.

In an attempt to gain further insight into citrin deficiency

and the development of CTLN2, we sought to construct an *Slc25a13*-knockout mouse model (hereto designated *Ctrn*-deficient mice). In the present study, we describe the phenotype of the *Ctrn*-deficient mice up to 1 year of age and specifically address the role of the AGC in aspects of the Mal-Asp NADH shuttle, gluconeogenesis, ureogenesis, and the NADH/NAD redox state. We also discuss the *Ctrn*-deficient mouse as a model for CTLN2.

MATERIALS AND METHODS

Generation of *Ctrn*-deficient mice. The targeting construct used to replace *Slc25a13* exon 10 was generated by using a combination of overlapping phage clones from an R1 embryonic stem (ES) cell-derived λ phage genomic library and PACs RP21-403P3 and RP21-616O22 isolated from a female (129S6/SvEvTac) mouse PAC library. The libraries were initially probed with *Slc25a13* cDNA clone MEλ1712 (2,172-bp *Eco*RI-*Hin*dIII fragment, nucleotides 463 to 2634) (45). The pPNT-SlcRX10 targeting vector consisted of a 1.7-kb short arm (incorporating *Bam*HI and *Eco*RI restriction sites by PCR) and a 3.4-kb long arm (incorporating *Xho*I restriction sites by PCR) and ultimately replaced a 347-bp region containing exon 10 with the 1,837-bp vector insert containing the neomycin resistance (*neo*) gene in the opposite orientation (Fig. 1A). The PCR-generated targeting probes (5′SlcP1.4 and 3′SlcP1.2) were designed from sequences lying outside of the genomic regions used to generate the vector arms.

The *Sal*I-linearized pPNT-SlcRX10 vector was electroporated into R1 ES cells and cultured under conditions of G418 (Geneticin; Invitrogen) and ganciclovir (Syntex) selection. Positively targeted clones, as determined by Southern blotting with probes 5′SlcP1.4 (*Xba*I digest) and 3′SlcP1.2 (*Msc*I digest) and a 0.6-kb *Pst*I fragment containing the 3′ end of the *neo* gene from the pPNT vector (NeoP0.6; *Afl*III digest), were independently aggregated with CD-1 blastocysts and reimplanted into pseudopregnant CD-1 foster mothers (28). Two clones gave rise to germ line-transmitting chimeras that were used for establishing 129Sv inbred and CD-1/129Sv mixed-background lines.

Genotyping. Mice were initially genotyped by Southern blotting (Fig. 1B, top panel) with probe 5′SlcP1.4 (*Xba*I digest) by using tail DNA prepared in Phase Lock Gel tubes (Eppendorf). A duplex PCR method (Fig. 1B, bottom panel) was later used with primers that recognize the integrated *neo* gene (5′-GAA GGA GCA AAG CTG CTA TTG GC-3′), *Slc25a13* exon 10 (5′-CTT TCT TCT GCA GCT CGC AGA GTC-3′), and the sequence within the long arm (5′-GAT CTA CCA AAC TAC CTT TGC AGA C-3′). Tail DNA used for duplex PCRs was prepared by a salting-out method for genomic DNA extraction (26).

Animal treatment. Mice were maintained on standard laboratory chow (Prolab RMH 1000) and analyzed at 8, 26, and 52 weeks of age. Eight- to 12-week-old mice were also subjected to ammonium chloride (NH_4Cl) injection (0.2 M solution; administered at 2 mmol per kg of body weight) as previously described (22). Sodium chloride (NaCl) injection (0.2 M solution; administered at 2 mmol per kg of body weight) was used as a control.

Northern blotting. Wild-type mRNA expression was determined by using a mouse multiple-tissue Northern blot (Clontech 7762-1). *Ctrn*-deficient mouse RNA expression was determined by using total RNA from 8- to 12-week-old mice prepared with Trizol reagent (Gibco) and Phase Lock Gel tubes (Eppendorf). Glyoxylated RNA (10 μg) was resolved on a 1.5% agarose gel, blotted, and probed as previously described (5, 42). To monitor the levels of RNA expression, cDNA probes for *Slc25a13* (1.3-kb *Not*I-*Eco*RI fragment, nucleotides 1737 to 3065; GenBank accession no. W77458), *Slc25a12* (2.1-kb *Not*I-*Eco*RI fragment, nucleotides 325 to 2471; accession no. AA881329), *Ass1* (0.5-kb *Hin*dIII-*Eco*RI fragment, nucleotides 158 to 681; accession no. AI226112), *PST1*/*Spink3* (359-bp fragment, nucleotides −44 to 315; determined by reverse transcription-PCR), and β-*actin* (provided by Clontech or using a 1,765-bp *Sal*I-*Not*I fragment, nucleotides 40 to 1884; accession no. BG077678) were used.

Western blotting. Protein extracts from 3-week-old *Ctrn*-deficient mice were prepared and electrophoretically separated, and citrin, ASS, and aralar proteins were detected by immunoblotting with antibodies as previously described (2). The anti-aralar antibody was a generous gift from J. Satrústegui, Universidad Autonoma de Madrid, Madrid, Spain.

Isolation of liver mitochondria. Liver mitochondria were isolated in a buffer containing 0.34 M sucrose, 100 mM KCl, 10 mM Tris-HCl (pH 7.4), and 1 mM EDTA essentially as previously described (9). Livers from 8- to 12-week-old mice were homogenized with a Teflon homogenizer. Following an initial spin at 3,000 rpm (Sorvall SS34 rotor), the mitochondria in the supernatant were washed twice
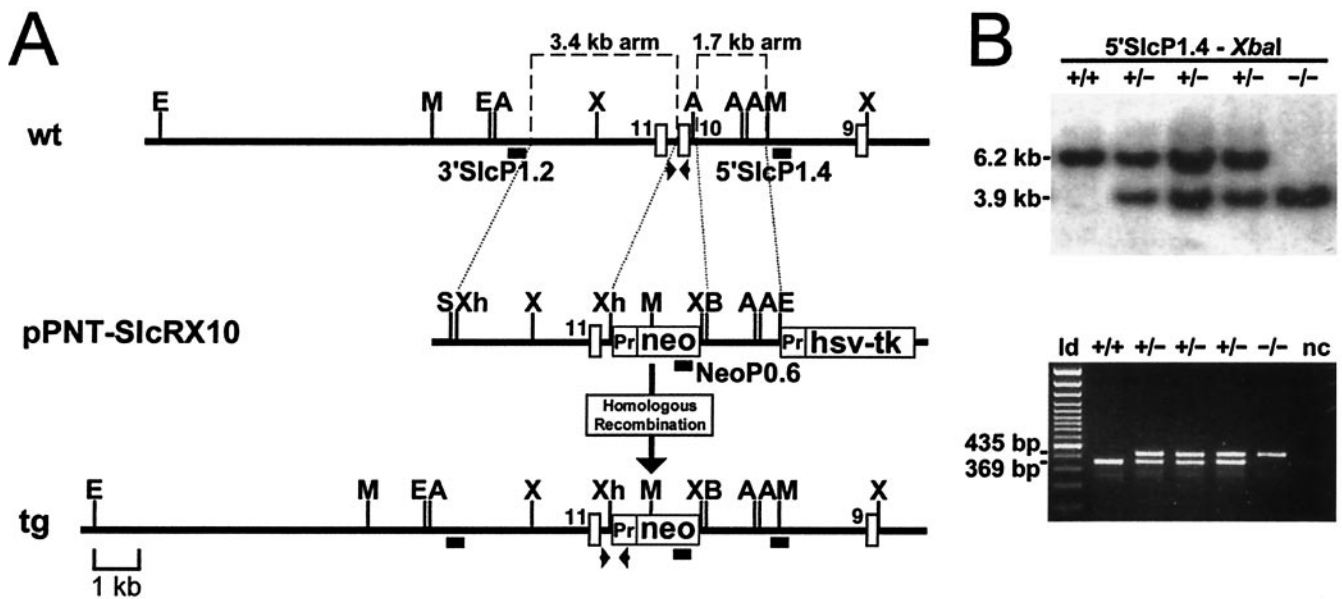
FIG. 1. Generation of *Ctrn*-deficient mice. (A) Targeting strategy for replacement of *Slc25a13* exon 10. The wild-type (wt) locus is shown, with the long (3.4-kb) and short (1.7-kb) arms used in the targeting vector (pPNT-SlcRX10) designated. Following homologous recombination, exon 10 was replaced with the neomycin resistance gene (*neo*; Pr, promoter) on the targeted allele (tg). Thymidine kinase from the herpes simplex virus (hsv-tk) was used for negative selection. Exons 9, 10, and 11 are depicted as white vertical boxes, probes are depicted by black horizontal boxes, and the PCR primers used for genotyping are indicated by horizontal arrowheads. A 1-kb scale is shown. A, *Afl*III; B, *Bam*HI; E, *Eco*RI; M, *Msc*I; S, *Sal*I; X, *Xba*I; Xh, *Xho*I. (B) Genotyping of *Ctrn*-deficient mice. Mice were genotyped by either Southern blotting with probe 5′SlcP1.4 (*Xba*I digest; separated on a 1% agarose gel) or by duplex PCR. Results for a representative litter containing wild-type (+/+), heterozygous (+/−), and homozygous (−/−) *Ctrn*-deficient mice are shown. For Southern blotting (top panel), both the wild-type (6.2-kb) and targeted (3.9-kb) alleles are visible. For the duplex PCR (bottom panel), primers situated within the *neo* gene, exon 10, and the long arm were used to amplify both the wild-type (369-bp) and targeted (435-bp) alleles and were visualized following separation on a 2% agarose gel. For the duplex PCR results, a 100-bp ladder (ld) and negative control (nc) are included.

by spins of 9,000 rpm, resuspended in a final volume of 0.5 to 1 ml of buffer per g of tissue, and used fresh for all experiments described.

Dynamic fluorimetry. Isolated mouse liver mitochondria were incubated in 1 mM phosphate buffer (pH 7.4) containing 80 mM KCl and 20 mM Tris-HCl (pH 7.4), essentially as previously described (1). The reaction volume was reduced to 1 ml and monitored in a quartz cuvette by using an Eppendorf fluorimeter at 37°C. An excitation wavelength below 340 nm and an emission reading above 400 nm were used. Mitochondria (100 μl of a 25 to 35 mg ml⁻¹ concentration) were initially added, followed by 2 μM carbonyl cyanide 4-trifluoro-methoxyphenyl-hydrazone (FCCP), 2 μM rotenone, 1 mM 2-oxoglutarate, 1 mM malonate, 1 mM Glu, and 1 mM Asp. The sample was mixed after the addition of each reagent.

Asp formation assay. Similar to the method described by LaNoue and Williamson (21), mitochondria (250 μl of a 25 to 35 mg ml⁻¹ concentration) were incubated in 10 ml of buffer (see "Dynamic fluorimetry" above) supplemented with 5 mM Glu, 5 mM Mal, and 2 mM ADP and incubated in 25-ml Erlenmeyer flasks in a metabolic shaker at 37°C. At various time points, two 1-ml samples (duplicates) were removed, immediately deproteinized with 50 μl of 1.6 M perchloric acid, and stored frozen until they were analyzed for the amount of Asp that was formed. Following a brief centrifugation to sediment the mitochondria, the amount of Asp within each sample was determined enzymatically as described previously (50).

Shuttle activity assays. Both Mal-Asp and α-glycerophosphate (α-GP) shuttle activities in mouse liver mitochondria were measured essentially as described by Scholz and Koppenhafer (43).

Liver perfusion. To measure the rate of gluconeogenesis, the rate of ureogenesis, and the lactate-to-pyruvate (L/P) ratio, liver perfusion was performed on 8- to 12-week-old *Ctrn*-deficient mice essentially as described previously (30). For the determination of gluconeogenesis, the mice were fasted prior to perfusion, and in the remaining experiments, the mice that were used were fed. After each mouse was anesthetized with an intraperitoneal injection of sodium pentobarbital (0.05 mg g of body weight⁻¹), the portal vein and inferior vena cava were cannulated, and the liver was perfused in situ with Krebs-Henseleit bicarbonate

buffer (pH 7.4, 37°C, saturated with 95% O₂–5% CO₂) by using a flowthrough method. The liver was perfused at a constant flow rate of approximately 8 ml min⁻¹. In each experiment, the liver was perfused for 30 min in the absence of exogenous substrates before various combinations of substrates were added (see Fig. 4). Perfusate was collected at appropriate times after passage through the liver.

Hepatic ammonia and amino acid levels. The freeze-clamped livers of 10- to 18-week-old mice were pulverized in liquid nitrogen, and the solute was extracted with 3% sulfosalicylic acid. The ammonia levels in the extracts were analyzed by flow injection (46) as described by Li et al. (22). The amino acid concentrations in the extracts were determined with a model 835 amino acid analyzer (Hitachi, Tokyo, Japan).

Protein determination. The protein concentrations of the mitochondrial fractions were determined by using the Lowry method with bovine serum albumin as a protein standard (23).

Statistical analysis. Statistical analysis was performed by using a two-tailed Student *t* test when two independent groups were compared, while a chi-square test for independence was used to determine the genotype and sex distributions within the population. A *P* value of <0.05 was considered statistically significant for all tests performed.

RESULTS

Generation of *Ctrn*-deficient mice. A combination of mouse genomic λ phage clones and PACs were used to assemble the genomic region encompassing exons 9 through 12 of the mouse *Slc25a13* locus (Fig. 1A). Based on sequence and genomic structural conservation between humans and mice, a strategy to replace exon 10, leaving exon 11 intact, was undertaken. The targeting rationale was based on two known CTLN2 mutations
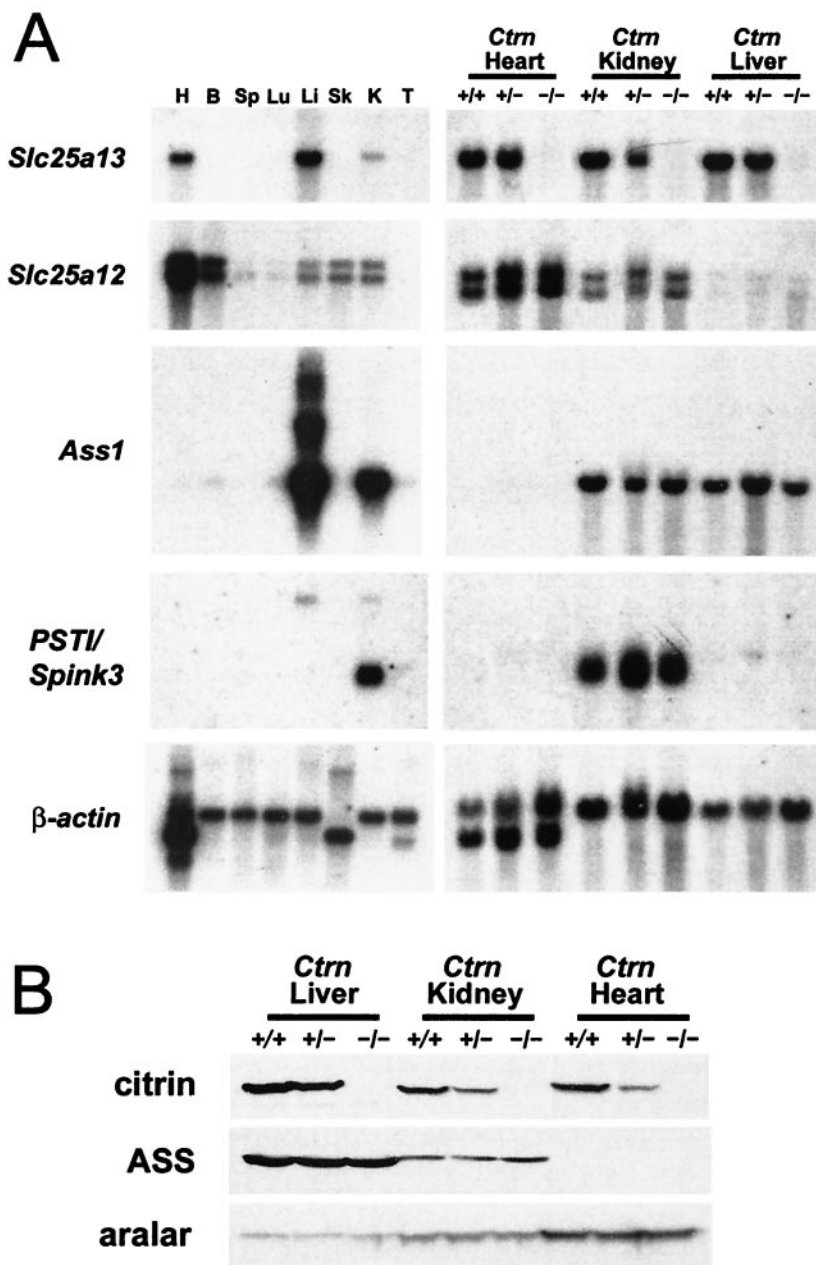
FIG. 2. Molecular characterization of *Ctrn*-deficient mice. (A) Northern blot analysis of RNA from various adult wild-type tissues (mRNA; left panels) as well as from the hearts, kidneys, and livers of 8- to 12-week-old *Ctrn*-deficient littermates (total RNA; right panels). Mouse cDNA probes for citrin (*Slc25a13*), aralar (*Slc25a12*), ASS (*Ass1*), PSTI (*PSTI/Spink3*), and β-actin were used. H, heart; B, brain; Sp, spleen; Lu, lung; Li, liver; Sk, skeletal muscle; K, kidney; T, testis. (B) Western blot analysis of liver, kidney, and heart protein extracts from 3-week-old *Ctrn*-deficient mice. Antibodies specific for citrin, ASS, and aralar were used.

(851del4 and S225X) predicted to truncate citrin prior to the first transmembrane domain (19).

ES cells that were electroporated with the pPNT-SlcRX10 vector were cultured under selection conditions and screened by Southern blotting by using targeting probes 5′SlcP1.4, 3′SlcP1.2, and NeoP0.6 (Fig. 1A). Following the confirmation of proper targeting, three clones were used in aggregation experiments, and chimeras were generated from two of the clones. Male chimeric mice were bred with both 129S1/SvImJ and CD-1 females. The offspring from these matings were

genotyped initially by Southern blotting and later by duplex PCR (Fig. 1B). CD-1/129Sv *Ctrn*-deficient mice were used for all experiments described, while the 129Sv inbred *Ctrn*-deficient mice were used for comparison studies in addition to studies that looked for subtle phenotypic effects more likely to be conspicuous in an inbred background.

Molecular characterization of the *Ctrn*-deficient mice. To confirm that the Slc25a13 gene had been knocked out, both mRNA and protein levels were measured (Fig. 2). The mRNA levels of *Slc25a13* were first confirmed in multiple tissues from

wild-type mice, and then RNA and protein levels were examined specifically in the livers, hearts, and kidneys of littermate *Ctrn*-deficient mice. Figure 2A shows that $Ctrn^{-/-}$ mice did not express *Slc25a13* RNA, indicating that the gene had indeed been knocked out. This was confirmed by Western blotting in which the targeted *Slc25a13* allele failed to produce any citrin-cross-reactive material, and hence the mutation in the $Ctrn^{-/-}$ mice was a null allele (Fig. 2B). Similar results have been found for the most common *SLC25A13* mutations in CTLN2 patients (53). Interestingly, although there was no change in the *Slc25a12* RNA or aralar protein expression levels within the livers, hearts, or kidneys of $Ctrn^{-/-}$ mice, low levels of *Slc25a12* and aralar were detected within the livers by Northern (Fig. 2A) and Western blot (Fig. 2B) analyses, respectively. Previous reports have failed to detect *Slc25a12* RNA expression in mouse liver (2, 10), but our findings are consistent with the presence of at least two *Slc25a12* expressed sequence tags in Unigene (www.ncbi.nlm.nih.gov/entrez/query.fcgi?db=unigene) that have been isolated from mouse liver.

Additionally, two other CTLN2-relevant genes were examined. The *Ass1* gene encodes the ASS enzyme in mice, while *PSTI/Spink3* is the mouse orthologue of the human PSTI gene. In CTLN2 patients, ASS protein is quantitatively reduced in the liver while ASS mRNA levels appear to be normal (17, 18). Furthermore, hepatic mRNA levels of the PSTI gene are upregulated in CTLN2 (16). An examination of the mice showed alterations in the expression patterns of ASS protein (Fig. 2B), *Ass1* RNA, and *PSTI/Spink3* RNA (Fig. 2A).

Morphology and viability of *Ctrn*-deficient mice. All $Ctrn^{-/-}$ mice appeared to be normal, healthy, fertile animals. Body weight, by gender, was similar across all *Ctrn* genotypes up to 1 year of age (latest time point examined). Hematoxylin-and-eosin-stained sections of all major tissues failed to reveal any gross structural changes (data not shown).

$Ctrn^{+/-}$ mice were interbred and produced the expected 1:2:1 ratio of wild-type, heterozygous, and homozygous offspring, on both the CD-1/129Sv mixed (263 animals analyzed) and 129Sv inbred (135 animals analyzed) backgrounds. Additionally, the sex ratio of males to females did not deviate statistically from the expected ratio of 1:1. During all of the studies, there was only a single recorded mortality due to unknown causes.

Biochemical characterization of *Ctrn*-deficient mice. (i) Asp transport. To investigate the extent to which Asp transport is abated in the livers of $Ctrn^{-/-}$ mice, two approaches were used: dynamic fluorimetry and assessment of Asp formation. Dynamic fluorimetry measures changes in the redox state of the intramitochondrial NAD(P)H pool due to the flux of metabolites into and out of the mitochondria. Once the mitochondrial NAD(P)H pool is poised in a reduced state, the rate of influx of Asp into the mitochondria (in the presence of 2-oxoglutarate) is then proportional to the rate of oxidation of the mitochondrial NAD(P)H pool observed, as oxaloacetate generated from Asp is reduced to Mal (1). A clear distinction in the rate of Asp influx, as measured by the rate of NAD(P)H oxidation, was observed for wild-type, $Ctrn^{+/-}$, and $Ctrn^{-/-}$ mice (Fig. 3A). While the phenotypic effects were clearly apparent, this method is dependent on substrate concentration, proceeds in the reverse direction, and does not take into account the electrogenic nature of the AGC. The second approach, assessment of Asp formation, was performed similarly to LaNoue and Williamson's (21) half-shuttle method in which mitochondria are incubated in a buffer containing Mal, Glu, and ADP. As shown in Fig. 3B, the formation of Asp generated from $Ctrn^{-/-}$ mouse liver mitochondria was statistically different from that observed for wild-type mice over the entire time course examined and statistically different from the formation observed for the $Ctrn^{+/-}$ mice at 10 and 15 min. The Asp generated from the mitochondria was subsequently shown to be specifically in the supernatant and not the mitochondria; this was confirmed by separating the mitochondria by centrifugation through a layer of silicone oil into a perchloric acid solution (data not shown). The overall decrease in Asp formation that was observed over the 15-min interval for all three mouse genotypes was most likely due to a combination of diminishing substrate and feedback inhibition of the accumulating ATP in the incubation buffer.

(ii) NADH shuttle activities. To investigate the role of citrin in the Mal-Asp shuttle, isolated liver mitochondria from *Ctrn*-deficient mice were assayed for their ability to perform the Mal-Asp and α-GP shuttles (Fig. 3C). The $Ctrn^{-/-}$ mice showed a drastic reduction in Mal-Asp shuttle activity compared to wild-type and $Ctrn^{+/-}$ mice, with $Ctrn^{+/-}$ mice also showing decreased Mal-Asp shuttle activity compared to that of wild-type mice. When the α-GP shuttle activity was measured, as expected, no difference was detected among the *Ctrn* genotypes. To ensure that there were no compensatory changes in the individual enzyme activities of either shuttle system in the absence of citrin, the activities of Mal dehydrogenase, Asp aminotransferase, and flavin-dependent GP dehydrogenase were measured and shown to be equivalent in the isolated liver mitochondria from all three *Ctrn* genotypes (data not shown).

(iii) Gluconeogenesis. To test the effects of citrin deficiency on gluconeogenesis, liver perfusions were performed in *Ctrn*-deficient mice with lactate and pyruvate as substrates. When 5 mM lactate was perfused through the livers of $Ctrn^{-/-}$ mice, a dramatically reduced ability to produce glucose was observed (Fig. 4A). Moreover, the $Ctrn^{+/-}$ mice showed an intermediate rate which was statistically different from those of both wild-type and $Ctrn^{-/-}$ mice. When pyruvate was used as a substrate (Fig. 4B), as expected, no difference in the rate of gluconeogenesis was seen among the three *Ctrn* genotypes. These results confirm that gluconeogenesis from reduced substrates (like lactate) specifically requires mitochondrial Asp efflux.

(iv) Ureogenesis. To investigate the extent to which ureogenesis is affected in the *Ctrn*-deficient mice, liver perfusion was also performed (Fig. 4C). Following the administration of 2 mM NH_4Cl, $Ctrn^{-/-}$ mice showed a dramatic reduction in the rate of urea production compared to those of both wild-type and $Ctrn^{+/-}$ mice. The addition of 2 mM Orn to stimulate the urea cycle did not seem to alleviate this effect; in fact, urea production went up in wild-type and $Ctrn^{+/-}$ mice while the rate of urea production remained unchanged in the $Ctrn^{-/-}$ mice. However, following the administration of 2 mM asparagine (Asn), an increase in the rate of urea production occurred in all mice, with the difference in rates of urea production between $Ctrn^{-/-}$ mice and both wild-type and $Ctrn^{+/-}$ mice being reduced but remaining statistically significant. The results suggest that Asp is limiting in the perfused livers and that
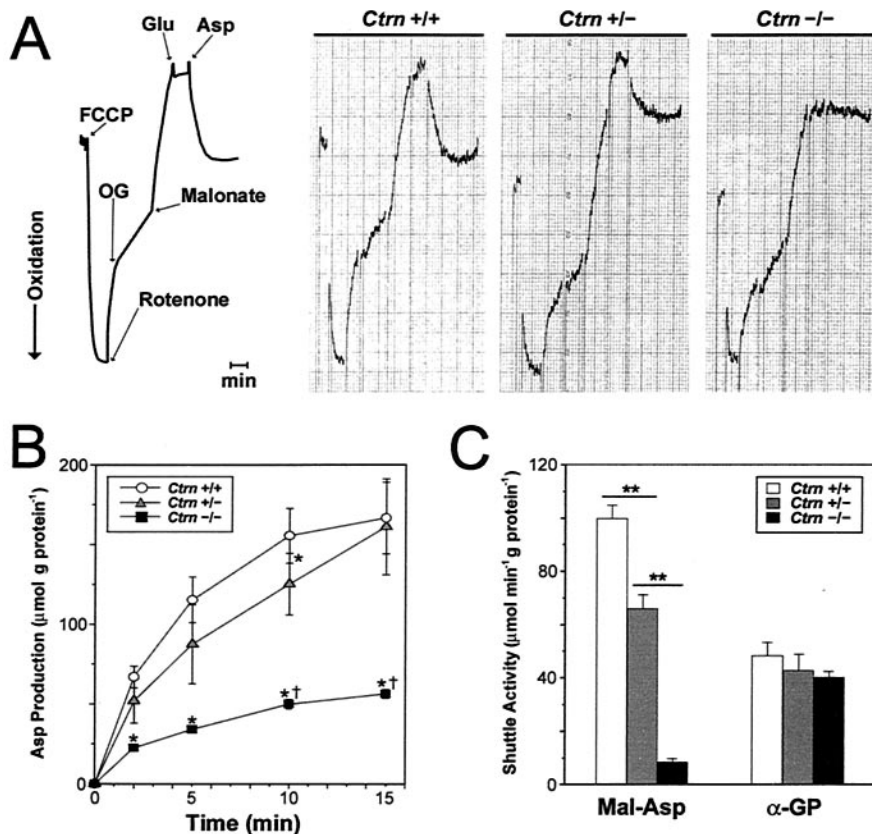
FIG. 3. Aspartate (Asp) transport and NADH shuttle activities of isolated liver mitochondria from *Ctrn*-deficient mice. (A) Dynamic fluorimetry monitoring Asp transport in *Ctrn*-deficient mouse liver mitochondria. The leftmost panel depicts the theoretical change in the redox state of the intramitochondrial NAD(P)H pool following the sequential addition of each substance indicated. The direction of oxidation along with a time scale (1 min) is shown. The three remaining panels show actual tracings of liver mitochondria generated from wild-type, $Ctrn^{+/-}$, and $Ctrn^{-/-}$ mice. OG, 2-oxoglutarate. (B) Asp formation over time following incubation of isolated *Ctrn*-deficient mouse liver mitochondria with Mal, Glu, and ADP. Standard error bars are included for each time point. Asterisks denote a statistically significant difference at a *P* value of <0.05 in results for either $Ctrn^{+/-}$ or $Ctrn^{-/-}$ mice and $Ctrn^{+/+}$ mice, while daggers denote a statistically significant difference at a *P* value of <0.05 in results for $Ctrn^{+/-}$ and $Ctrn^{-/-}$ mice. (C) Mal-Asp and α-GP NADH shuttle activities in isolated *Ctrn*-deficient mouse liver mitochondria. Standard error bars are indicated. Asterisks denote a statistically significant difference at a *P* value of <0.01 in results between genotypes.

Asn can partially mitigate the effects of citrin's absence on ureogenesis as observed in the $Ctrn^{-/-}$ mice.

(v) L/P ratio. To investigate the effect of citrin deficiency on the hepatic NADH/NAD redox state, the L/P ratio was measured in the perfused livers of *Ctrn*-deficient mice (Fig. 4D). The results show that the hepatocyte L/P ratio in $Ctrn^{-/-}$ mice was increased compared to those of both wild-type and $Ctrn^{+/-}$ mice following the administration of 2 mM NH₄Cl. When 2 mM Orn was added to the perfusate, the L/P ratio in both wild-type and $Ctrn^{+/-}$ mice increased to levels similar to those observed for the $Ctrn^{-/-}$ mice. However, following the administration of 2 mM Asn, the L/P ratios in wild-type and $Ctrn^{+/-}$ mice returned to baseline levels while the ratio in $Ctrn^{-/-}$ mice remained significantly higher under these conditions. These results confirm that Asp is limiting in the perfused livers, but in this case, Asn cannot alleviate the requirements of mitochondrial Asp in translocating NADH into the mitochondria of $Ctrn^{-/-}$ mice.

Hepatic ammonia and amino acid metabolism following NH₄Cl treatment. To specifically test hepatic ammonia metabolism in the *Ctrn*-deficient mice, the liver specimens were ex-

amined 10 min after an NH₄Cl injection. Interestingly, differences were seen in the hepatic ammonia levels of $Ctrn^{-/-}$ mice compared to those of wild-type and $Ctrn^{+/-}$ littermates independent of NH₄Cl injection (Fig. 5A). This suggests that $Ctrn^{-/-}$ mice normally maintain hepatic ammonia levels that are elevated compared to those of wild-type and $Ctrn^{+/-}$ mice, and this may be due to a decreased ability for ammonia disposal.

Intrahepatic levels of Glu, glutamine (Gln), Asp, and Orn plus Cit plus Arg (as a measure of urea cycle function) were also analyzed 10 min after injection (Fig. 5B). Differences in intrahepatic Glu levels are evident for $Ctrn^{-/-}$ mice and their wild-type and $Ctrn^{+/-}$ littermates independent of NH₄Cl injection; this difference is similar to that observed for the intrahepatic ammonia levels. Following the NH₄Cl injection, however, the $Ctrn^{+/-}$ mice showed elevations in the liver Glu levels similar to those of the $Ctrn^{-/-}$ mice. Differences were also seen in Gln levels; after the NH₄Cl injection, a decrease in Gln levels was observed in mice of all genotypes, while the elevated Gln levels seen in the $Ctrn^{-/-}$ mice compared to those of the wild-type or $Ctrn^{+/-}$ mice were conserved. The combined levels of the amino acids involved in the urea cycle were elevated
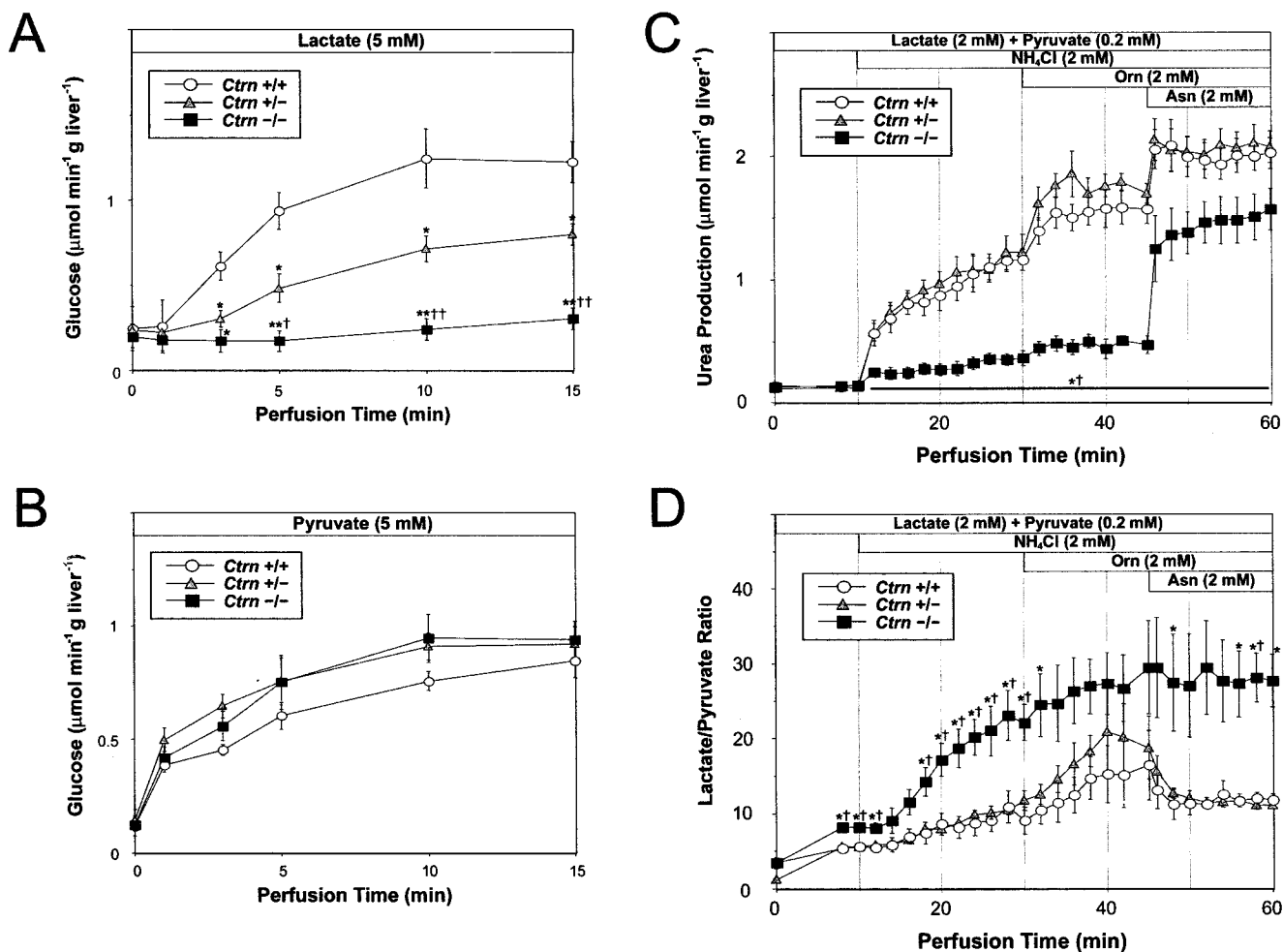
FIG. 4. Liver perfusion of *Ctrn*-deficient mice. Glucose production was measured by liver perfusion with lactate (A) and pyruvate (B) as substrates, while ureogenesis (C) and the L/P ratio (D) were measured by perfusion with lactate, pyruvate, and NH_4Cl, followed by Orn and Asn. Eight- to 12-week-old mice were used for all studies. Standard error bars are included for each time point. Asterisks denote a statistically significant difference at a *P* value of <0.05 (*) or <0.01 (**) in results for either *Ctrn*^{+/-} or *Ctrn*^{-/-} mice and *Ctrn*^{+/+} mice, while daggers denote a statistically significant difference at a *P* value of <0.05 (†) or <0.01 (††) in results for *Ctrn*^{+/-} and *Ctrn*^{-/-} mice.

after the NH_4Cl injection in mice of all *Ctrn* genotypes. Despite this elevation, no differences were detected among wild-type, *Ctrn*^{+/-}, or *Ctrn*^{-/-} mice within either injection group. Finally, following the NH_4Cl injection, the liver Asp values were decreased in wild-type and *Ctrn*^{+/-} mice (the change in *Ctrn*^{+/-} mice was not statistically significant). This trend did not hold true for the *Ctrn*^{-/-} mice, in which the liver Asp values appeared to remain unchanged after the NH_4Cl injection, resulting in a statistically significant difference between *Ctrn*^{-/-} mice and both wild-type and *Ctrn*^{+/-} mice. Calculating the ratio of Asp to Glu in the livers of the mice, after either NaCl or NH_4Cl injection, we clearly found a lower Asp/Glu ratio in the *Ctrn*^{-/-} mice, which may indicate a difficulty in converting Glu to Asp.

DISCUSSION

A defect in mitochondrial Asp export due to the loss of citrin function may be predicted to lead to alterations in the path-ways of the Mal-Asp NADH shuttle and the NADH/NAD redox state, as well as gluconeogenesis and ureogenesis (4, 20, 25, 51). Our investigations show that the Asp efflux from liver mitochondria was decreased at least threefold in *Ctrn*^{-/-} mice compared to that of the wild-type mice, translating to a 10-fold decrease in the Mal-Asp NADH shuttle activity. The rates of gluconeogenesis from lactate and ureogenesis from NH_4Cl were also significantly affected. Despite the absence of citrin, however, residual Asp efflux resulted in measurable residual Mal-Asp shuttle activity and presumably contributed to the residual rates of gluconeogenesis from lactate and ureogenesis in the *Ctrn*^{-/-} mice. Unlike results of previous reports (2, 10), low-level *Slc25a12* mRNA and aralar protein expression was found within the mouse liver, possibly contributing to the residual Asp transport measured. It remains to be tested whether aralar is solely responsible for this residual rate of Asp transport in *Ctrn*^{-/-} mice.

Despite the measurable deficits in AGC-dependent path-ways, the *Ctrn*^{-/-} mice failed to show any significant physio-
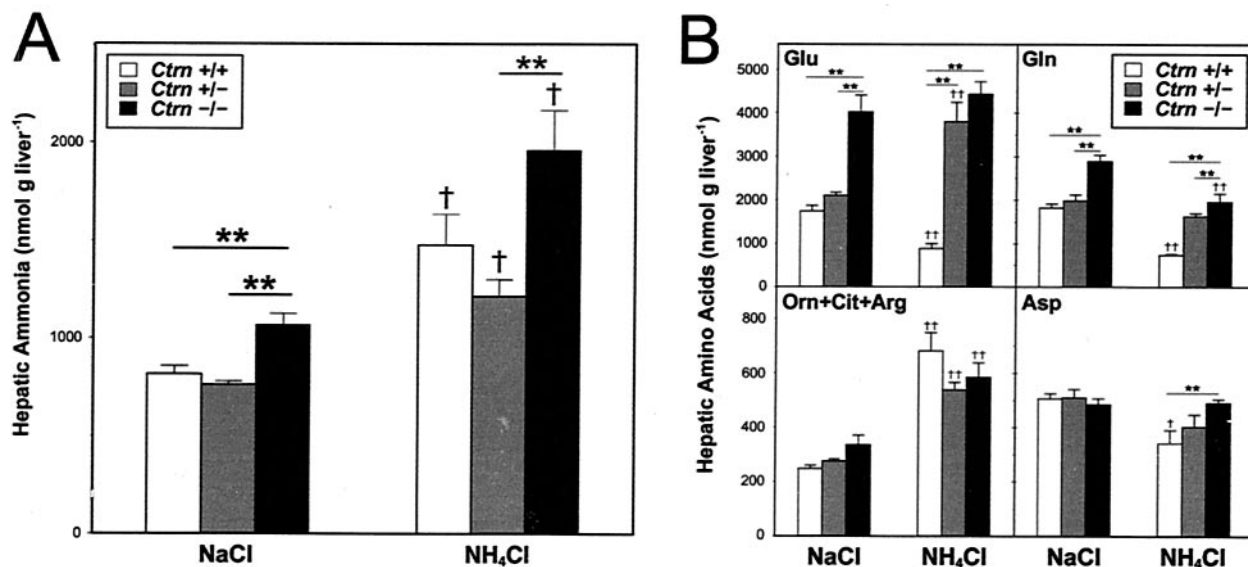
FIG. 5. Hepatic ammonia and amino acid levels following nitrogen loading in *Ctrn*-deficient mice. Measurements of ammonia (A) and amino acids (B) in the liver following freeze-clamping performed 10 min after intraperitoneal injection of either NaCl (control) or ammonium chloride (NH₄Cl; 2 mmol per kg of body weight of 8- to 12-week-old mice) solutions. Asterisks indicate a statistically significant difference at a *P* value of <0.01 in results for genotypes within the same treatment group, while daggers indicate statistically significant differences at *P* values of <0.05 (†) and <0.01 (††) in results for the same genotype within different treatment groups.

logical consequences. For the Mal-Asp shuttle activity specifically, the lack of any obvious compensatory up-regulation of α-GP shuttle activity, or of the intramitochondrial enzymatic activities for either shuttle, suggests that the livers of the *Ctrn⁻/⁻* mice can sufficiently transport reducing equivalents under normal physiological conditions. For gluconeogenesis, comparable levels of glucose and lactate in serum found in wild-type and *Ctrn⁻/⁻* mice suggest that gluconeogenesis from lactate is not significantly impaired (data not shown). Furthermore, preliminary evidence suggests that even after overnight fasting, serum glucose levels in *Ctrn⁻/⁻* mice do not differ from those in wild-type littermates. Further studies under extreme fasting conditions or prolonged exercise may help to uncover a stronger phenotype.

For ureogenesis, the initial rate of urea production, which was lower in *Ctrn⁻/⁻* mice than in wild-type mice, was partially ameliorated by the addition of Asn to the liver perfusate. It is known that Asn can serve as a source of cytoplasmic Asp through the asparaginase reaction (20, 44), suggesting that Asp, in general, was a limiting factor that partially contributed to the reduced rate of urea production seen in the *Ctrn⁻/⁻* mice. Serological measures of plasma ammonia and blood urea nitrogen levels showed no observable differences between wild-type and *Ctrn⁻/⁻* mice, and surprisingly, the *Ctrn⁻/⁻* mice responded to increased protein loads in their diet by increasing the urea output and maintaining serum ammonia levels (data not shown). This suggests that mitochondrial Asp, despite previous reports about its preferential use for the ASS reaction (25), is probably not an essential source in mice. Finally, the observation of only minor alterations in hepatic ammonia and amino acid metabolism following NH₄Cl injection suggests that, despite significant nitrogen loading, changes in amino

acid levels for the derivation of cytosolic sources of Asp may be sufficient to maintain proper urea cycle functioning.

Our original goal for creating the *Ctrn*-deficient mice was to establish a mouse model of CTLN2. From our study, however, it has become clear that *Slc25a13* mutations alone may not be sufficient in producing a CTLN2-like phenotype, despite the complete absence of citrin function. Although some CTLN2 patients have been shown to have only a small decrease in ASS activity compared to that of controls (53), the majority of cases show ≤15% of control values (13), which is likely responsible for the hyperammonemia and citrullinemia observed clinically. The *Ctrn⁻/⁻* mice failed to show signs of CTLN2 (i.e., hyperammonemia and alterations in serum amino acids) most likely due to the normal hepatic ASS activity that was observed (data not shown). Recently, Imamura et al. (12) reported finding two siblings who were homozygous for the *SLC25A13* mutations: one presenting with CTLN2 symptoms, and the other remaining symptom free. Measurement of their hepatic ASS activities revealed that the younger, clinically affected sibling had 2% of control values, while the older sibling possessed 20% of control values. Although this may suggest that the loss of ASS activity could be progressive over time, additional genetic or environmental factors are likely required for the onset of CTLN2 symptoms. Therefore, lack of evidence for the loss of ASS activity within the liver of *Ctrn⁻/⁻* mice up to 1 year of age suggests that additional factors may also be required for the onset of a CTLN2-like phenotype in mice.

Although differences in the life spans of humans and mice may explain why the *Ctrn⁻/⁻* mice failed to show a hepatic loss of ASS, species-specific differences in gene regulation are perhaps a more plausible explanation for the lack of a phenotype. The residual Asp transport observed in the *Ctrn⁻/⁻* mice may

be unique to mice, as *SLC25A12* expression does not appear to present in human liver (19). Additional evidence for this claim comes from the lack of Unigene *SLC25A12* cDNAs (expressed sequence tag) derived solely from human liver. In addition, the loss of Mal-Asp shuttle activity may have different consequences in CTLN2 patients than in *Ctrn*$^{-/-}$ mice. In humans, the α-GP shuttle is not thought to play a significant role within the liver, as human liver exhibits less than 1/20 of the flavin-dependent GP dehydrogenase activity of rodents (33). This last observation suggests that the transport of reducing equivalents in the human liver may be heavily dependent on the Mal-citrate shuttle in the absence of a functional Mal-Asp shuttle, resulting in the creation of acetyl-coenzyme A and stimulating fatty acid synthesis. The fat accumulation that has been observed in the livers of some patients with citrin deficiencies (both NICCD and CTLN2) may be the result of such a process (11, 12, 47–49). Nevertheless, the *Ctrn*-deficient mice will be useful in the future in order to investigate the metabolic differences in the NADH shuttles of humans and mice, to identify specific genetic and/or environmental triggers that lead to reduced hepatic ASS levels and to a CTLN2 onset, and consequently to establish a suitable model of human CTLN2.

ACKNOWLEDGMENTS

REFERENCES

1. **Azzi, A., J. B. Chappell, and B. H. Robinson.** 1967. Penetration of the mitochondrial membrane by glutamate and aspartate. Biochem. Biophys. Res. Commun. **29:**148–152.
2. **Begum, L., M. A. Jalil, K. Kobayashi, M. Iijima, M. X. Li, T. Yasuda, M. Horiuchi, A. del Arco, J. Satrústegui, and T. Saheki.** 2002. Expression of three mitochondrial solute carriers, citrin, aralar1 and ornithine transporter, in relation to urea cycle in mice. Biochim. Biophys. Acta **1574:**283–292.
3. **Ben-Shalom, E., K. Kobayashi, A. Shaag, T. Yasuda, H. Z. Gao, T. Saheki, C. Bachmann, and O. Elpeleg.** 2002. Infantile citrullinemia caused by citrin deficiency with increased dibasic amino acids. Mol. Genet. Metab. **77:**202–208.
4. **Borst, P.** 1963. Hydrogen transport and transport metabolites, p. 137–162. *In* P. Karson (ed.), Funktionelle und morphologische Organization der Zelle. Springer-Verlag KG, Heidelberg, Germany.
5. **Burnett, W. V.** 1997. Northern blotting of RNA denatured in glyoxal without buffer recirculation. BioTechniques **22:**668–671.
6. **del Arco, A., M. Agudo, and J. Satrústegui.** 2000. Characterization of a second member of the subfamily of calcium-binding mitochondrial carriers expressed in human non-excitable tissues. Biochem. J. **345:**725–732.
7. **del Arco, A., and J. Satrústegui.** 1998. Molecular cloning of aralar, a new member of the mitochondrial carrier superfamily that binds calcium and is present in human muscle and brain. J. Biol. Chem. **273:**23327–23334.
8. **Gao, H. Z., K. Kobayashi, A. Tabata, H. Tsuge, M. Iijima, T. Yasuda, H. S. Kalkanoglu, A. Dursun, A. Tokatli, T. Coskun, F. K. Trefz, D. Skladal, H. Mandel, J. Seidel, S. Kodama, S. Shirane, T. Ichida, S. Makino, M. Yoshino, J. H. Kang, M. Mizuguchi, B. A. Barshop, S. Fuchinoue, S. Seneca, S. Zeesman, I. Knerr, M. Rodes, P. Wasant, I. Yoshida, L. De Meirleir, M. Abdul Jalil, L. Begum, M. Horiuchi, N. Katunuma, S. Nakagawa, and T. Saheki.** 2003. Identification of 16 novel mutations in the argininosuccinate synthetase gene and genotype-phenotype correlation in 38 classical citrullinemia patients. Hum. Mutat. **22:**24–34.
9. **Hogeboom, G. H.** 1955. Fractionation of cell components of animal tissues. Methods Enzymol. **I:**16–19.
10. **Iijima, M., A. Jalil, L. Begum, T. Yasuda, N. Yamaguchi, M. Xian Li, N. Kawada, H. Endou, K. Kobayashi, and T. Saheki.** 2001. Pathogenesis of adult-onset type II citrullinemia caused by deficiency of citrin, a mitochondrial solute carrier protein: tissue and subcellular localization of citrin. Adv. Enzyme Regul. **41:**325–342.
11. **Ikeda, S., M. Yazaki, Y. Takei, T. Ikegami, Y. Hashikura, S. Kawasaki, M. Iwai, K. Kobayashi, and T. Saheki.** 2001. Type II (adult onset) citrullinaemia: clinical pictures and the therapeutic effect of liver transplantation. J. Neurol. Neurosurg. Psychiatry **71:**663–670.
12. **Imamura, Y., K. Kobayashi, T. Shibatou, S. Aburada, K. Tahara, O. Kubozono, and T. Saheki.** 2003. Effectiveness of carbohydrate-restricted diet and arginine granules therapy for adult-onset type II citrullinemia: a case report of siblings showing homozygous SLC25A13 mutation with and without the disease. Hepatol. Res. **26:**68–72.
13. **Kobayashi, K., M. Horiuchi, and T. Saheki.** 1997. Pancreatic secretory trypsin inhibitor as a diagnostic marker for adult-onset type II citrullinemia. Hepatology **25:**1160–1165.
14. **Kobayashi, K., M. Iijima, T. Yasuda, D. S. Sinasac, N. Yamaguchi, L.-C. Tsui, S. W. Scherer, and T. Saheki.** 2000. Type II citrullinemia (citrin deficiency): a mysterious disease caused by a defect of calcium-binding mitochondrial carrier protein, p. 565–587. *In* R. Pochet, R. Donato, J. Haiech, C. W. Heizmann, and V. Gerke (ed.), Calcium: the molecular basis of calcium action in biology and medicine. Kluwer Academic Publishers, Dordrecht, The Netherlands.
15. **Kobayashi, K., M. J. Jackson, D. B. Tick, W. E. O'Brien, and A. L. Beaudet.** 1990. Heterogeneity of mutations in argininosuccinate synthetase causing human citrullinemia. J. Biol. Chem. **265:**11361–11367.
16. **Kobayashi, K., M. Nakata, H. Terazono, T. Shinsato, and T. Saheki.** 1995. Pancreatic secretory trypsin inhibitor gene is highly expressed in the liver of adult-onset type II citrullinemia. FEBS Lett. **372:**69–73.
17. **Kobayashi, K., T. Saheki, Y. Imamura, T. Noda, I. Inoue, S. Matuo, S. Hagihara, H. Nomiyama, Y. Jinno, and K. Shimada.** 1986. Messenger RNA coding for argininosuccinate synthetase in citrullinemia. Am. J. Hum. Genet. **38:**667–680.
18. **Kobayashi, K., N. Shaheen, R. Kumashiro, K. Tanikawa, W. E. O'Brien, A. L. Beaudet, and T. Saheki.** 1993. A search for the primary abnormality in adult-onset type II citrullinemia. Am. J. Hum. Genet. **53:**1024–1030.
19. **Kobayashi, K., D. S. Sinasac, M. Iijima, A. P. Boright, L. Begum, J. R. Lee, T. Yasuda, S. Ikeda, R. Hirano, M. A. Crackower, I. Kondo, L. C. Tsui, S. W. Scherer, and T. Saheki.** 1999. The gene mutated in adult-onset type II citrullinaemia encodes a putative mitochondrial carrier protein. Nat. Genet. **22:**159–163.
20. **Krebs, H. A., P. Lund, and M. Stubbs.** 1976. Interrelations between gluconeogenesis and urea synthesis, p. 269–291. *In* R. W. Hanson, M. A. Mehlman, and H. A. Lardy (ed.), Gluconeogenesis, its regulation in mammalian species. Wiley, New York, N.Y.
21. **LaNoue, K. F., and J. R. Williamson.** 1971. Interrelationships between malate-aspartate shuttle and citric acid cycle in rat heart mitochondria. Metabolism **20:**119–140.
22. **Li, M. X., T. Nakajima, T. Fukushige, K. Kobayashi, N. Seiler, and T. Saheki.** 1999. Aberrations of ammonia metabolism in ornithine carbamoyl-transferase-deficient spf-ash mice and their prevention by treatment with urea cycle intermediate amino acids and an ornithine aminotransferase inactivator. Biochim. Biophys. Acta **1455:**1–11.
23. **Lowry, O. H., N. J. Rosebrough, A. L. Farr, and R. J. Randall.** 1951. Protein measurement with the Folin phenol reagent. J. Biol. Chem. **193:**265–275.
24. **McMurray, W. C., F. Mohyuddin, R. J. Rossiter, J. C. Rathburn, G. H. Valentine, S. J. Koegler, and D. E. Zarfas.** 1962. Citrullinemia: a new aminoaciduria associated with mental retardation. Lancet **1:**138.
25. **Meijer, A. J., J. A. Gimpel, G. Deleeuw, M. E. Tischler, J. M. Tager, and J. R. Williamson.** 1978. Interrelationships between gluconeogenesis and ureogenesis in isolated hepatocytes. J. Biol. Chem. **253:**2308–2320.
26. **Miller, S. A., D. D. Dykes, and H. F. Polesky.** 1988. A simple salting out procedure for extracting DNA from human nucleated cells. Nucleic Acids Res. **16:**1215.
27. **Nagata, N., I. Matsuda, and K. Oyanagi.** 1991. Estimated frequency of urea cycle enzymopathies in Japan. Am. J. Med. Genet. **39:**228–229.
28. **Nagy, A., J. Rossant, R. Nagy, W. Abramow-Newerly, and J. C. Roder.** 1993. Derivation of completely cell culture-derived mice from early-passage embryonic stem cells. Proc. Natl. Acad. Sci. USA **90:**8424–8428.
29. **Naito, E., M. Ito, S. Matsuura, Yokota, T. Saijo, Y. Ogawa, S. Kitamura, K. Kobayashi, T. Saheki, Y. Nishimura, N. Sakura, and Y. Kuroda.** 2002. Type II citrullinaemia (citrin deficiency) in a neonate with hypergalactosaemia detected by mass screening. J. Inherit. Metab. Dis. **25:**71–76.
30. **Nakajima, T., M. Horiuchi, H. Yamanaka, Z. Kizaki, F. Inoue, N. Kodo, A. Kinugasa, T. Saheki, and T. Sawada.** 1997. The effect of carnitine on ketogenesis in perfused livers from juvenile visceral steatosis mice with systemic carnitine deficiency. Pediatr. Res. **42:**108–113.
31. **Ohura, T., K. Kobayashi, Y. Tazawa, I. Nishi, D. Abukawa, O. Sakamoto, K. Iinuma, and T. Saheki.** 2001. Neonatal presentation of adult-onset type II citrullinemia. Hum. Genet. **108:**87–90.
32. **Palmieri, L., B. Pardo, F. M. Lasorsa, A. del Arco, K. Kobayashi, M. Iijima, M. J. Runswick, J. E. Walker, T. Saheki, J. Satrústegui, and F. Palmieri.** 2001. Citrin and aralar1 are Ca^{2+}-stimulated aspartate/glutamate transporters in mitochondria. EMBO J. **20:**5060–5069.
33. **Sadava, D., M. Depper, M. Gilbert, B. Bernard, and E. R. McCabe.** 1987. Development of enzymes of glycerol metabolism in human fetal liver. Biol. Neonate **52:**26–32.

34. **Saheki, T., and K. Kobayashi.** 2002. Mitochondrial aspartate glutamate carrier (citrin) deficiency as the cause of adult-onset type II citrullinemia (CTLN2) and idiopathic neonatal hepatitis (NICCD). J. Hum. Genet. **47:** 333–341.

35. **Saheki, T., K. Kobayashi, and I. Inoue.** 1987. Hereditary disorders of the urea cycle in man: biochemical and molecular approaches. Rev. Physiol. Biochem. Pharmacol. **108:**21–68.

36. **Saheki, T., K. Kobayashi, I. Inoue, S. Matuo, S. Hagihara, and T. Noda.** 1987. Increased urinary excretion of argininosuccinate in type II citrullinemia. Clin. Chim. Acta **170:**297–304.

37. **Saheki, T., K. Kobayashi, T. Miura, S. Hashimoto, Y. Ueno, T. Yamasaki, H. Araki, H. Nara, Y. Shiozaki, Y. Sameshima, M. Suzuki, Y. Yamauchi, Y. Sakazume, K. Akiyama, and Y. Yamamura.** 1986. Serum amino acid pattern of type II citrullinemic patients and effect of oral administration of citrulline. J. Clin. Biochem. Nutr. **1:**129–142.

38. **Saheki, T., M. Sase, K. Nakano, and Y. Yagi.** 1985. Arginine metabolism in citrullinemic patients, p. 149–158. *In* A. Mori, B. D. Cohen, and A. Lowenthal (ed.), Guanidines. Plenum Press, New York, N.Y.

39. **Saheki, T., A. Ueda, M. Hosoya, K. Kusumi, S. Takada, M. Tsuda, and T. Katsunuma.** 1981. Qualitative and quantitative abnormalities of argininosuccinate synthetase in citrullinemia. Clin. Chim. Acta **109:**325–335.

40. **Saheki, T., A. Ueda, M. Hosoya, M. Sase, K. Nakano, and T. Katsunuma.** 1983. Enzymatic analysis of citrullinemia (12 cases) in Japan. Adv. Exp. Med. Biol. **153:**63–76.

41. **Saheki, T., A. Ueda, K. Iizima, N. Yamada, K. Kobayashi, K. Takahashi, and T. Katsunuma.** 1982. Argininosuccinate synthetase activity in cultured skin fibroblasts of citrullinemic patients. Clin. Chim. Acta **118:**93–97.

42. **Sambrook, J., and D. W. Russell.** 2001. Molecular cloning: a laboratory manual, 3rd ed. Cold Spring Harbor Laboratory Press, Cold Spring Harbor, N.Y.

43. **Scholz, T. D., and S. L. Koppenhafer.** 1995. Reducing equivalent shuttles in developing porcine myocardium: enhanced capacity in the newborn heart. Pediatr. Res. **38:**221–227.

44. **Shiota, M., M. Hiramatsu, Y. Fujimoto, M. Moriyama, K. Kimura, M. Ohta, and T. Sugano.** 1994. The capacity of the malate-aspartate shuttle differs between periportal and perivenous hepatocytes from rats. Arch. Biochem. Biophys. **308:**349–356.

45. **Sinasac, D. S., M. A. Crackower, J. R. Lee, K. Kobayashi, T. Saheki, S. W. Scherer, and L. C. Tsui.** 1999. Genomic structure of the adult-onset type II citrullinemia gene, SLC25A13, and cloning and expression of its mouse homologue. Genomics **62:**289–292.

46. **Svensson, G., and T. Anfalt.** 1982. Rapid determination of ammonia in whole blood and plasma using flow injection analysis. Clin. Chim. Acta **119:**7–14.

47. **Tamamori, A., Y. Okano, H. Ozaki, A. Fujimoto, M. Kajiwara, K. Fukuda, K. Kobayashi, T. Saheki, Y. Tagami, and T. Yamano.** 2002. Neonatal intrahepatic cholestasis caused by citrin deficiency: severe hepatic dysfunction in an infant requiring liver transplantation. Eur. J. Pediatr. **161:**609–613.

48. **Tazawa, Y., K. Kobayashi, T. Ohura, D. Abukawa, F. Nishinomiya, Y. Hosoda, M. Yamashita, I. Nagata, Y. Kono, T. Yasuda, N. Yamaguchi, and T. Saheki.** 2001. Infantile cholestatic jaundice associated with adult-onset type II citrullinemia. J. Pediatr. **138:**735–740.

49. **Tomomasa, T., K. Kobayashi, H. Kaneko, H. Shimura, T. Fukusato, M. Tabata, Y. Inoue, S. Ohwada, M. Kasahara, Y. Morishita, M. Kimura, T. Saheki, and A. Morikawa.** 2001. Possible clinical and histologic manifestations of adult-onset type II citrullinemia in early infancy. J. Pediatr. **138:**741–743.

50. **Williamson, J. R., and B. E. Corkey.** 1969. Assays of intermediates of the citric acid cycle and related compounds by fluorometric enzyme methods, p. 434–509. *In* J. M. Lowenstein (ed.), Methods in enzymology: citric acid cycle. Academic Press, New York, N.Y.

51. **Williamson, J. R., B. Safer, K. F. LaNoue, C. M. Smith, and E. Walajtys.** 1973. Mitochondrial-cytosolic interactions in cardiac tissue: role of the malate-aspartate cycle in the removal of glycolytic NADH from the cytosol. Symp. Soc. Exp. Biol. **27:**241–281.

52. **Yamaguchi, N., K. Kobayashi, T. Yasuda, I. Nishi, M. Iijima, M. Nakagawa, M. Osame, I. Kondo, and T. Saheki.** 2002. Screening of SLC25A13 mutations in early and late onset patients with citrin deficiency and in the Japanese population: identification of two novel mutations and establishment of multiple DNA diagnosis methods for nine mutations. Hum. Mutat. **19:**122–130.

53. **Yasuda, T., N. Yamaguchi, K. Kobayashi, I. Nishi, H. Horinouchi, M. A. Jalil, M. X. Li, M. Ushikai, M. Iijima, I. Kondo, and T. Saheki.** 2000. Identification of two novel mutations in the SLC25A13 gene and detection of seven mutations in 102 patients with adult-onset type II citrullinemia. Hum. Genet. **107:**537–545.